Geophysical Research Letters

Water level (m) above m.s.l

Water level changes (cm)

Interferogram (phase)

Backscatter amplitude
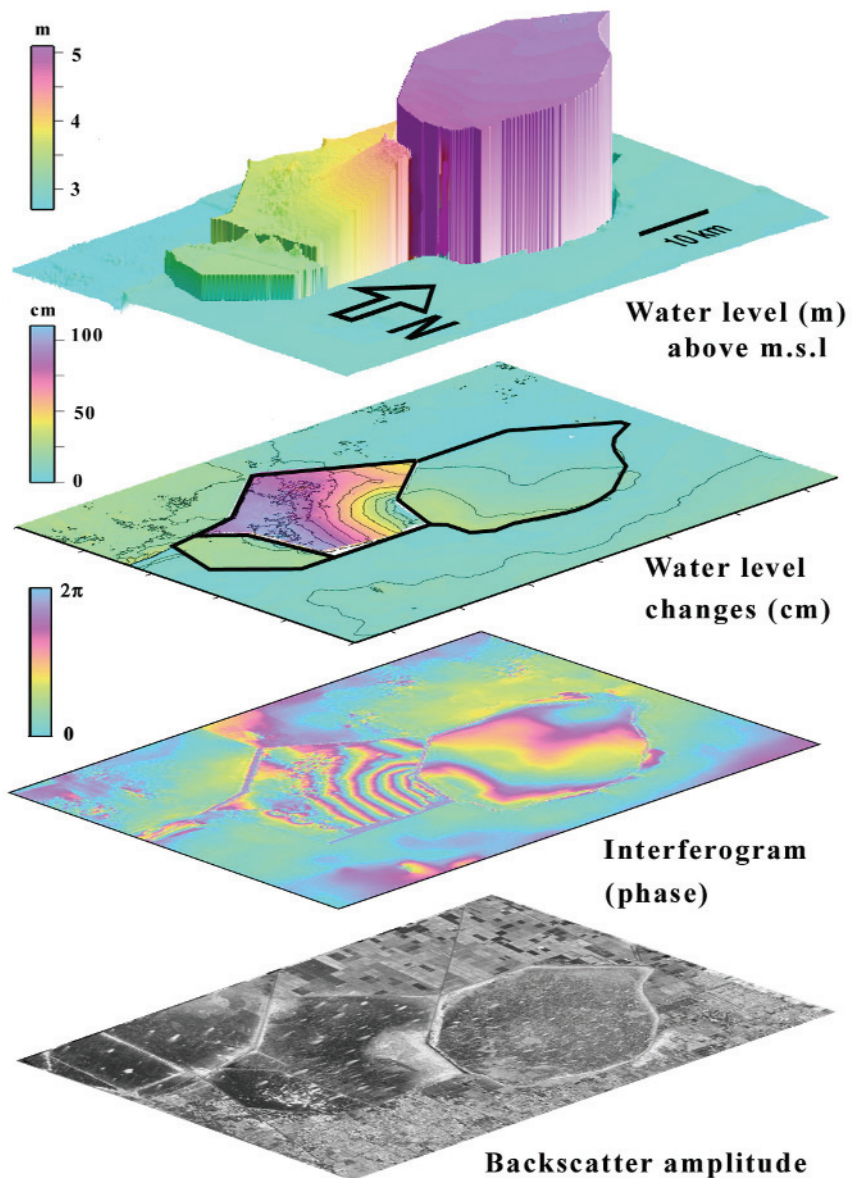
Observing the Everglades water levels from space • Kinetic model measures plasma flow on Titan • Part 2 of the special section on the San Andreas Fault Observatory project

Space-based measurements of sheet-flow characteristics in the Everglades wetland, Florida

Shimon Wdowinski,[1,2] Falk Amelung,[1] Fernando Miralles-Wilhelm,[3] Timothy H. Dixon,[1] and Richard Carande[4]

[1] New space-based observations of South Florida with interferometric SAR (InSAR) reveal spatially detailed, quantitative images of water levels in the Everglades. The new data capture dynamic water level topography, providing the first detailed picture of wetland sheet flow. We observe localized radial sheet flow in addition to well-known southward unidirectional sheet flow, modelled as a linear diffusive flow. We obtain quantitative estimates of flow diffusivity ($23-91$ m^2/s), the first space-based estimates of such hydrologic parameter for the Everglades. Space-based hydrologic observations can provide critical information for monitoring, understanding and managing wetland sheet flow, and contribute to wetland restoration. *INDEX TERMS:* 1243 Geodesy and Gravity: Space geodetic surveys; 1294 Geodesy and Gravity: Instruments and techniques; 1860 Hydrology: Runoff and streamflow; 1890 Hydrology: Wetlands; 1894 Hydrology: Instruments and techniques. **Citation:** Wdowinski, S., F. Amelung, F. Miralles-Wilhelm, T. H. Dixon, and R. Carande (2004), Space-based measurements of sheet-flow characteristics in the Everglades wetland, Florida, *Geophys. Res. Lett.*, *31*, L15503, doi:10.1029/2004GL020383.

1. Introduction

[2] The Everglades region of south Florida (Figure 1a) is an excellent example of a critical wetlands habitat that has been degraded due to human activity. Restoration of this habitat is currently underway, and will eventually include restoring natural hydroperiod, the cyclic rise and fall of water levels in response to seasonal rainfall variation, to which native species are well adapted (loss of natural hydroperiod has resulted in loss of habitat and significant decline of native species). Hydroperiod restoration is complicated by the presence of a dense network of levees, control channels and flood gates, and large spatial variations in flow resistance due to these man-made features as well as natural and invasive vegetation. In this paper we demonstrate the ability to obtain high accuracy ($5-10$ cm), high spatial resolution (300×300 m^2) measurements of Everglades' water level from space, using Interferometric SAR (InSAR).

The spatial resolution is nearly a two order of magnitude improvement on existing ground-based techniques, sufficient to constrain hydrologic models and obtain quantitative estimates flow diffusivity and friction.
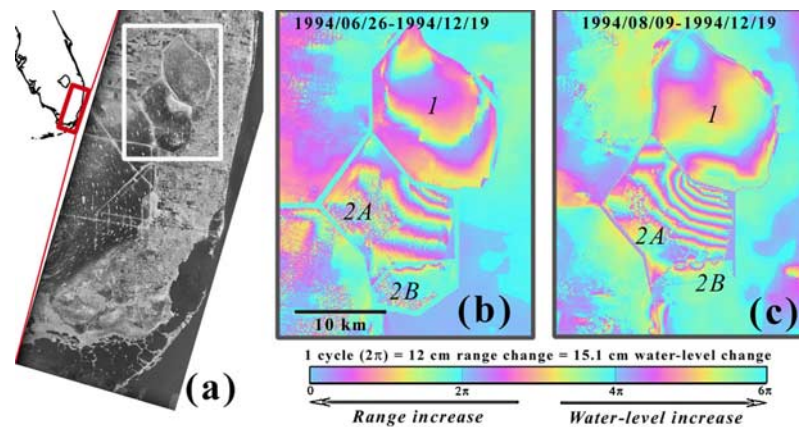
2. InSAR Data

[3] Our data are derived from Synthetic Aperture Radar (SAR) data acquired by the Japan Earth Resources Satellite (JERS-1), processed using interferometric methods [*Massonnet and Feigl*, 1998]. JERS-1 operated an L-band (1.275 Ghz frequency, 24 cm wavelength) SAR during $1992-1998$ with 75-km swath and 18 m resolution. *Alsdorf et al.* [2000] first demonstrated that interferometric processing of L-band SAR data acquired at different times could detect changes in wetlands water levels with a precision of $1-3$ cm. Given the presence of emergent vegetation, the radar pulse is backscattered twice ("double-bounce" [*Richards et al.*, 1987]), from the water surface and vegetation. A change in water level between the two acquisitions results in a change in travel time for the radar signal (range change), recorded as a phase change in the interferogram. In this approach, only the change between the two data acquisitions is known; the actual water level at either time is unknown, hampering hydrologic modelling.

[4] Our data consist of three SAR passes over South Florida acquired in 1994 (1994/6/24, 1994/8/9, and 1994/12/19), at the beginning, middle, and end of the local wet season (June–November). We calculated 3 interferograms, spanning 44 days (June–August), 132 days (August–December), and 176 days (June–December) (the last two are shown in Figure 1). The interferogram calculations include phase unwrapping, but not topographic phase removal (south Florida topography is flat). Interferogram baselines range from $214-647$ m. The raw interferograms show various coherence levels in rural and urban areas. We applied a spatial filter to improve interferogram quality, which slightly degrades horizontal resolution (100×100 to 300×300 m^2), still significantly better than available terrestrial monitoring. All the observed phase changes (colors in Figure 1) can be attributed to surface changes (they correlate with surface features) and hence are unlikely to be due to atmospheric effects [*Zebker et al.*, 1997]. Each phase cycle (2π) corresponds to 12 cm of displacement in the radar line-of-sight, or 15.1 cm of vertical displacement. Lateral phase changes over wetlands reflect water level changes.

3. InSAR Detected Water Level Changes

[5] The most significant elevation changes occur in the northern section of the interferogram, across man-made

[1]Division of Marine Geology and Geophysics, University of Miami, Miami, Florida, USA.
[2]Also at Department of Geophysics and Planetary Sciences, Raymond and Beverly Sackler Faculty of Exact Sciences, Tel Aviv University, Ramat Aviv, Israel.
[3]Department of Civil, Architectural and Environmental Engineering, University of Miami, Coral Gables, Florida, USA.
[4]Vexcel Corporation, Boulder, Colorado, USA.

Figure 1. L-band backscatter amplitude and interferograms of southern Florida. (a) JERS backscatter of eastern south Florida showing the study area. (b) 176-day (June–December) interferogram. (c) 132-day (August–December) interferogram. Labels 1, 2A, and 2B refer to Water Conservation Areas.

structures known as Water Conservation Areas (WCA) 1, 2A, and 2B. These areas are located roughly half way between Lake Okeechobee and the Gulf of Mexico, the beginning and end of the Everglades flow. They provide significant ecological, water storage and flood control benefits to the region as well as important wildlife habitat. The WCAs are separated by a series of levees. The surface water flows south through a series of gates, some are shown in Figure 2a.

[6] Figure 1 shows the L-band backscatter amplitude and two interferograms. The amplitude (brightness) represents the radar backscatter, which depends on surface dielectric properties and orientation with respect to the satellite. The small, elongated white areas are vegetated tree islands [*Sklar and Van Der Valk*, 2003] aligned with the long-term regional flow direction. The large white zones in 2A and 2B are densely vegetated. The interferograms show that water level changes are unidirectional in the eastern section of area 2A and radial in the western part. The change in Figure 1b indicates water level decrease towards the NE by about 60 cm (4 cycles) and in Figure 1c a NE decrease of about 105 cm (7 cycles). Both interferograms also show in the northern edge of area 2B water level change characterized by 3 radial ("bulls-eye") patterns (Figures 1b and 1c).
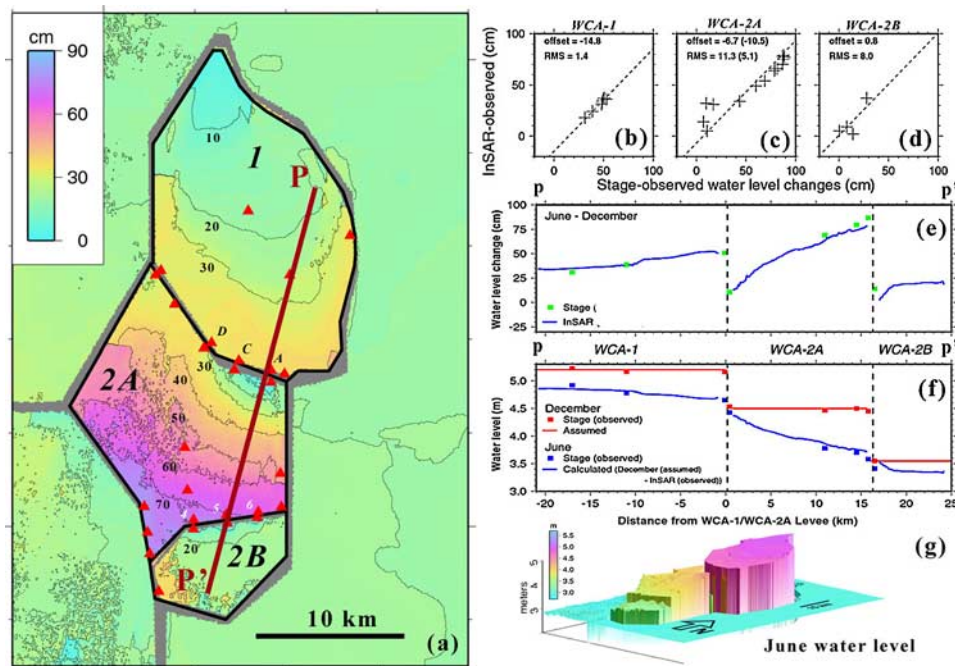
[7] Figure 2 shows the June–December water level changes in areas 1, 2A, 2B and surroundings. Because InSAR measures relative changes within each area, but not between the areas, we assigned in each area the lowest change level to zero. The most significant water level changes occur in the eastern section of area 2A, where water level changes can be described by a series of NWN-ESE nearly parallel contours. The water level changes are illustrated in a profile along maximum slope in the eastern part of the WCA (brown lines in Figure 2a). The profile (solid blue line in Figure 2e) shows a southward increase in water level change in all areas. The overall gradient and shorter wavelength variations vary. The highest gradient is in 2A, whereas in area 2B high gradient occurs only near the levee; further south the change gradient is very small.

[8] The InSAR data can be compared observations with ground (stage) data, which consist of daily average level above the NGVD29 datum (red triangles in Figure 2a). The stage data are from the South Florida Water Management District's DBHYDRO database (http://www.sfwmd.gov/org/ema/dbhydro/index.html). We use these data to calculate water level differences between the two SAR acquisition dates. The InSAR values are calculated from the nearest pixels to the stage station. Most of the stage stations are located along levees, where the InSAR data is less reliable due to the edge effect of our spatial filter. The InSAR-based water level changes reflect a wider area and in some cases are a few hundreds meter away from the actual location of the stage stations. Nevertheless the agreement is quite good, as indicated by the low root-mean-square (rms) deviation from the line with slope 1, which was calculated using a least-square analysis (Figures 2b, 2c, and 2d). The calculated offset and rms in area 2A (Figure 2c) are biased by two outliers. Figure 2c shows the estimated rms difference with (11.3 cm) and without (5.1 cm) these outliers. Area 2B has a small number of stage measurements with limited geographic distribution, but nevertheless shows reasonable agreement (8.0 cm rms). The same least-square analysis with the other two interferograms (June–August and August–December), gives very similar rms values, suggesting that the accuracy of the InSAR water level change measurements is 5–10 cm and the precision is better than this. This procedure also allows us to compute and correct the datum offset between stage and InSAR data, which is arbitrarily set to zero at the lowest level in each area.

4. From Water Level Change to Absolute Water Level

[9] The new space-based observations provide, with very high spatial resolution, water level changes in the Everglades over 44–176 day time intervals. Because these time intervals are long compared to the duration of natural and man-made water level changes in the Everglades (days to several weeks), the observed water level changes represent the difference between two water levels and should not be interpreted as a continuous process (average height change). Nevertheless it is possible to calculate absolute water levels (above mean sea level) at specific times, as follows. Figure 2f presents stage elevations during June and

Figure 2. (a) InSAR-based water level change map for the June–December time interval of areas 1, 2A and 2B. Black lines mark levees separating the areas. Red triangles mark location of stage stations. Brown line marks water level profile perpendicular to water level contours. The characters (A, C, D, 4, 5 and 6) mark the location of gates S-10A, S-10C, S-10D, 144, 145 and 146, respectively. The numbers (10, 20, …, 70) label contours of water level changes. (b, c, and d) Comparison between the zero-offset InSAR and the stage data calculated separately for each area. The bracket values in (c) are obtained after removing two outliers (located above the dashed line). (e) Comparison between InSAR and stage water level changes along the profile (after offset correction). Stage data observed in the centre of areas 1 and 2A are projected onto the profile. (f) June and December water levels along the profile. (g) Three-dimensional illustration of June water level, calculated by subtracting the corrected InSAR data from the assumed flat December levels, for the entire study area.

December. The December InSAR observation occurred during a period of negligible water flow, resulting in almost flat water levels in the three areas (red lines in Figure 2f). By using the December stage data as a reference level, we can calculate the June water levels (Figure 2g). Sample profiles (blue lines) agree well with available stage data for the two time periods. We repeat the same procedure with the August–December interferogram to obtain the August water levels.

[10] The InSAR observations therefore represent snapshots of dynamic water topography during the June and August data acquisitions. The dynamic topography is dominated by gate operations, allowing water to flow from area 1 to 2A and from 2A to 2B (Figure 2). Using gate flow information, we can correlate and explain the relations between the observed topography and flow rate. For example, the three small bull-eye patterns in the north of area 2B reflect low flow rates across gates 145, 146 and 147 (Figure 2). A more detailed explanation of dynamic topography in area 2A is now provided.

5. Model

[11] Given the spatially detailed water height estimates at specific times, we can derive some key parameters specific to the Everglades environment, using a linearized diffusion flow model [Akan and Yen, 1981]. This diffusion flow approximation is derived from conservation of mass and momentum principles, neglecting inertial terms in the latter. The model is appropriate to low-Reynolds hydrologic flows, where the flow is predominantly laminar. It follows the same formulation as the SFWMM [Lal, 1998, 2000] which has been used extensively to model surface flow in South Florida. The diffusion flow approximation entails a Fickian form for the relation between the volumetric flow rate (Q) and the surface water elevation (H) gradient, i.e., $Q = -D\partial H/\partial x$; where D is flow diffusivity. For instance, if Manning's friction relationship is applied, then $D = h^{5/3}/(n|\partial H/\partial x|^{1/2})$ [Lal, 1998, 2000], where h is a reference averaged water depth, and n is Manning's friction coefficient (dimensionless), a measure of the resistance to flow [Lal, 1998, 2000].

[12] In order to calculate dynamically supported water levels, we need to specify initial and boundary conditions, which are poorly constrained. Rather than modelling water levels in all three water conservation areas and accounting for complex gate operation history, we focus on the process that governs dynamically supported water level topography and model the region where this phenomenon is most pronounced - the eastern section of area 2A (Figure 2a). In this region the hydrologic flow lines are orthogonal to InSAR water level contours, indicating a southward flow during June and August 1994. The unidirectional flow in this region is amenable to a simple one-dimensional

analytical solution. As a first approximation, we: (1) assume a spatially uniform flow diffusivity (D); and (2) neglect sink terms (horizontal flow rates $\gg$ net lateral and/or vertical inflow rates such as rainfall and/or evaporation), deriving the familiar one-dimensional diffusion equation:
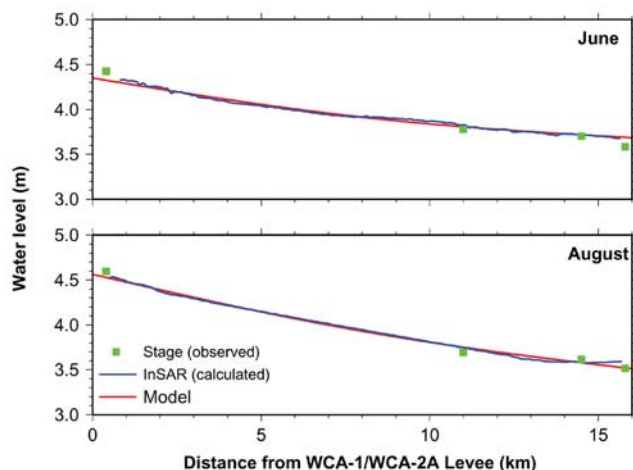
$$\frac{\partial H}{\partial t} = D\frac{\partial^2 H}{\partial x^2} \qquad (1)$$

The initial and boundary conditions are derived from the stage and gate operation time series. We apply an instantaneous gate opening model, which assumes (1) a flat water level in area 2A prior to the opening of the gates, (2) water level in area 1 remains constant and (3) water level at southern end of area 2A remains constant. All three assumptions are approximations to stage data. The above assumptions allow us to determine initial and boundary conditions and to solve equation (1) both analytically [*Carslaw and Jaeger*, 1959] and numerically. We use the analytical solution with a best-fit adjustment to estimate the two flow parameters and their uncertainties: the initial water elevation difference across the gate (H_0) and the flow characteristic length $(Dt)^{1/2}$.

[13] Figure 3 and Table 1 show that the InSAR data constrain the model parameters to ~5% uncertainty. However, the full coupling of time and flow diffusivity as a single parameter - the diffusion characteristic length $(Dt)^{1/2}$ - does not allow us to uniquely determine the flow diffusivity (D). Nevertheless, we use the gate operation history to estimate the time since opening, as 16 ± 2 days for June and 8 ± 2 days for August, in order to estimate this parameter. The different water levels in June and August (Table 1) allow us to relate calculated flow diffusivity to water level variations.

6. Wetland Sheet-Flow Characteristics

[14] Table 1 shows estimated model parameters for June and August 1994. Our results indicate that the August flow

Table 1. Summary of Hydrologic Modeling (see Figure 3)

Parameter	Description	June 1994	August 1994
H_0 (m)	Elevation difference	0.66 ± 0.04	1.05 ± 0.05
Dt (m^2)	(Characteristic length)^2	$3.68 \pm 0.12 \times 10^7$	$4.74 \pm 0.15 \times 10^7$
D (m^2/s)	Flow diffusivity	27 ± 4	75 ± 16
n^a	Manning's friction coefficient	$1.1 - 2.3$	$0.9 - 1.2$

[a] n is estimated using reference values of $h = 0.6-0.8$ m and $\partial H/\partial x = 4 - 7 \times 10^{-5}$.

resulted from a higher water elevation difference across the gate (H_0) than in June. It also suggests that the diffusion characteristic length $(Dt)^{1/2}$ is 25–30% higher in August than in June. However, the large time (since gate opening) difference between the two observations yields a significant difference between our estimated flow diffusivity (D), 27 ± 4 m^2/s in June and 75 ± 16 m^2/s in August. This large estimate difference partly reflects the limitation of our 1-D model. Nevertheless it provides the first large scale flow diffusivity estimate that is based on actual observations. To our knowledge, the only other regional scale estimate of the Everglades diffusivity is given by *Lal* [2000], who obtained his estimate by assuming water depth $h \approx 1$ m, slope $\partial H/\partial x \approx -2 \times 10^{-5}$ and Manning friction coefficient $n \approx 1$.

[15] We also calculate the corresponding Manning friction coefficient n for diffusive flow [*Lal*, 1998]. Reported values of n for sheet flow through vegetation [e.g., *Lal*, 2000; *Nepf*, 1999; *Lee et al.*, 1999] are in the range $0.1 < n < 1.0$. Our large-scale InSAR estimates are higher. For June, n is higher ($1.1-2.3$) compared to August ($0.9-1.2$). The large difference between the two estimates may reflect the limitations of our model. Nevertheless, our results suggest a higher flow resistance in June at lower water levels than in August, suggesting the influence of vegetation. Decreasing resistance to flow with increasing water depths has been observed before [e.g., *Lee et al.*, 1999]. This is also consistent with estimated decreases of $1-2$ orders of magnitude in scalar transport dispersion between unvegetated and vegetated surface flows [*Nepf*, 1999].

[16] In summary, L-band InSAR can measure water levels in the Everglades and other wetlands with high spatial resolution and a vertical precision of $5-10$ cm. These data can be used in an operational sense to better understand the flow regime, and can also yield high-resolution estimates of important physical flow properties, e.g., flow diffusivity. These in turn can be used to spatially and temporally characterize the flow associated with different soil types, vegetation coverage and land use, and better manage these important wetland environments.

Figure 3. Comparison between observed stage, InSAR, and best-fit modeled water levels in June and August 1994 across area 2A (along the N-S profile shown in Figure 2). Model parameters are described in Table 1.

References

Akan, A. O., and B. C. Yen (1981), Diffusion-wave flood routing in channel networks, *J. Hydraul. Div. Am. Soc. Civ. Eng.*, *107*, 719–731.

Alsdorf, D. E., et al. (2000), Interferometric radar measurements of water level changes on the Amazon flood plain, *Nature*, *404*, 174–177.

Carslaw, H. S., and J. C. Jaeger (1959), *Conduction of Heat in Solids*, 2nd ed., Oxford Univ. Press, New York.

Lal, A. M. W. (1998), Performance comparison of overland flow algorithms, *J. Hydraul. Eng.*, *124*, 342–349.

Lal, A. M. W. (2000), Numerical errors in groundwater and overland flow models, *Water Resour. Res.*, *36*, 1237–1247.

Lee, J. K., V. Carter, and N. B. Rybicki (1999), Determining flow-resistance coefficients in the Florida Everglades, paper presented at Third International Symposium on Ecohydraulics, Int. Assoc. for Hydraul. Res., Salt Lake City, Utah.

Massonnet, D., and K. L. Feigl (1998), Radar interferometry and its application to changes in the Earth's surface, *Rev. Geophys.*, *36*, 441–500.

Nepf, H. M. (1999), Drag, turbulence, and diffusion in flow through emergent vegetation, *Water Resour. Res.*, *35*, 479–489.

Richards, L. A., P. W. Woodgate, and A. K. Skidmore (1987), An explanation of enhanced radar backscattering from flooded forests, *Int. J. Remote Sens.*, *8*, 1093.

Sklar, F. H., and A. Van Der Valk (Eds.) (2003), *Tree Islands of the Everglades*, pp. 1–552, Kluwer Acad., Norwell, Mass.

Zebker, H. A., P. A. Rosen, and S. Hensley (1997), Atmospheric effects in interferometric synthetic aperture radar surface deformation and topographic maps, *J. Geophys. Res.*, *102*, 7547–7563.

————————————

F. Amelung, T. H. Dixon, and S. Wdowinski, Division of Marine Geology and Geophysics, University of Miami, 4600 Rickenbacker Causeway, Miami, FL 33149-1098, USA. (shimonw@rsmas.miami.edu)

R. Carande, Vexcel Corporation, Boulder, CO, USA.

F. Miralles-Wilhelm, Department of Civil, Architectural and Environmental Engineering, University of Miami, Coral Gables, FL, USA.